

Bank Conflict Free Comparison-based Sorting On GPUs

Nodari Sitchinava¹ and Volker Weichert²

¹ University of Hawaii, Manoa, HI, USA

² Goethe University Frankfurt am Main, Frankfurt, Germany

Abstract. In this paper we present a framework for designing algorithms in shared memory of GPUs without incurring memory bank conflicts. Using our framework we develop the first comparison-based shared memory sorting algorithm that incurs no bank conflicts. It can be used as a subroutine for GPU sorting algorithms to replace current use of sorting networks in shared memory. Using our bank conflict free shared memory sorting subroutine as a black box, we design BCFMergesort, an algorithm for merging sorted streams of data that are larger than shared memory. Our algorithm performs all accesses to global memory in coalesced manner and incurs no bank conflicts during the merge.

1 Introduction

During the past decade GPUs – the massively parallel processors developed for graphics rendering – have been adapted for general purpose computation and CUDA and OpenCL – extensions for C programming language – have been developed for programming them. With hundreds of cores capable of running thousands of threads, GPUs have become a standard computational platform in high-performance computing (HPC) and have been successfully used to analyze data in natural sciences, such as biology, chemistry, physics and astronomy.

1.1 Brief introduction to GPU organization

To manage the large number of cores, GPUs are designed hierarchically. They consist of the GPU’s on-board memory, known as *global memory*, and a number of *streaming multiprocessors (SMs)*. Each SM consists of multiple *scalar processors*, or *cores*, and several types of faster but smaller memories.

Each physical core can support multiple threads. The management of so many threads comes with a very specific thread organization. All threads on a GPU are organized into *warps* – a collection of 32 threads – which must execute code as a *single-instruction, multiple data (SIMD)* processor in an implicitly

Work supported in part by the DFG grant ME 2088/3-1 within the priority programme SPP 1736 (Algorithms for Big Data) and by the Danish National Research Foundation grant DNRF84 through Center for Massive Data Algorithmics (MADALGO).

synchronized (lock-step) manner. SIMD execution implies that any if statement that requires some subset of threads to execute one instruction, while another subset to execute another instruction, will result in the two subsets of threads waiting for each other. This is known as *branch divergence* in GPU literature and can result in drastic loss of parallelism for nested conditional statements.

Warps are grouped into *cooperative thread arrays (CTAs)*, also known as *thread blocks*. All warps of a CTA must execute the same code, are run asynchronously from each other with the ability to call explicit barrier synchronizations. All warps of a CTA are guaranteed to be run on the same physical SM. Finally, synchronization across multiple CTAs can be performed using explicit barriers.

The memory of a GPU is organized into multiple memory types each with its own advantages, but also their own challenges.

- *Global memory* is the largest but the slowest of all memory types. To hide the latency associated with access to global memory, GPU programmers are encouraged to *coalesce* their accesses to global memory. The accesses are coalesced when the threads of a warp access contiguous address space in the global memory. Global memory is accessible by all threads running on the GPU at all times and the programmer is responsible to ensure the correctness of the data under concurrent updates in such an asynchronous setting.
- *Shared memory* is faster but also smaller than global memory. It does not require coalesced accesses, however, it is organized into a limited number of memory banks. Each thread can access any memory bank, however, simultaneous accesses to the same memory bank by multiple threads of a warp cause a contention, known in GPU literature as *bank conflicts*. The threads causing a bank conflict are serviced sequentially resulting in the loss of parallelism. Each CTA implements its own address space within shared memory and the data in shared memory is exclusive to all threads of a single CTA, i.e., the threads of one CTA cannot access the data of another CTA via shared memory.
- *Registers* are the fastest type of memory on GPUs. Efficient access to data stored in registers does not require coalescing, nor does it suffer from memory bank conflicts. However, registers are private to each thread, very limited in size (only 63 of them per thread on our NVIDIA GTX 580 graphics card) and the addressing must be exactly the same for all threads of a warp. If more registers are required by a thread, the excess is stored in *local memory*.
- *Local memory* is not a separate physical memory type, but instead is implemented as a logical partition of global memory. However, the latency of accessing slow global memory is mitigated by automatic caching of recently used data of local memory in the same memory banks where shared memory resides.
- *Texture memory* and *Constant memory* are other types of memory which are very useful in graphics rendering applications. However they are very specialized and their use for general purpose computations is very poorly understood. In this paper we do not use those memories.

1.2 Effects of bank conflicts on runtime

Due to large latency of accessing global memory, fast practical implementations typically first load data into shared memory and process data from there. Efficient access to contiguous data in global memory through coalescing is well understood and Merrill and Grimshaw [10] has optimized the process to get sustainable throughput that are close to theoretical maximal.

However, once the data in shared memory, the access patterns in the presence of banked memory is less understood.

To observe the effects of bank conflicts on runtime, consider the problem of *colored prefix sums*: given an array of N elements and a set of d colors $\{c_1, c_2, \dots, c_d\}$, with a color c_i associated with each element, colored prefix sums asks to compute d independent prefix sums among the elements of the same color.

Given $P \ll N$ processors, colored prefix sums can be solved using the standard three phase approach to solving prefix sums: partition the input into P subsets of contiguous N/P elements and compute the d sums (one for each color) within each subset using an independent processor; compute d independent prefix sums on the d sets of P values each from previous phase; finally add the value of the appropriate color from the previous step while computing the prefix sum within the subsets for each of d colors using independent processor per subset. If $P \ll N$ the runtime of the second step is negligible (in practice it is typically performed using a single processor) and the algorithm is dominated by the first and the third step of the algorithm. If the second step takes negligible time and $d \ll N/P$, the runtime should vary little as a function of d .

Figure 1a (dashed line) shows the actual runtime of colored prefix sums. Unlike our prediction, we can see that it grows significantly as a function of d . Figure 1b shows the runtime of just the third phase and the number of bank conflicts incurred during execution. One can clearly see a correlation between the two. After implemented an improved version of colored prefix sums that does not incur any bank conflicts (see Appendix A for implementation details), one can see that the runtime of the third phase indeed becomes constant as a function of d (solid lines). This simple example demonstrates that if we want to be able to accurately predict runtimes of GPU algorithms using asymptotic analysis, it is very important to design algorithms without any bank conflicts.

1.3 Past work on sorting on GPUs

Sorting numbers in an array was one of the first combinatorial problems implemented on GPUs. Purcel et al. [14] were the first to implement a bitonic sorting network on a GPU, while Sintorn et al. [17] implemented the first sorting algorithm in the CUDA programming environment. Since then many different algorithms have been implemented on GPUs, e.g. mergesort [15,5,18], quicksort [4], bitonic sort [13], radixsort [11] and samplesort [9].

For comparison-based algorithms, when data is small enough, fast implementations typically implement a sorting network (usually Batcher's odd-even

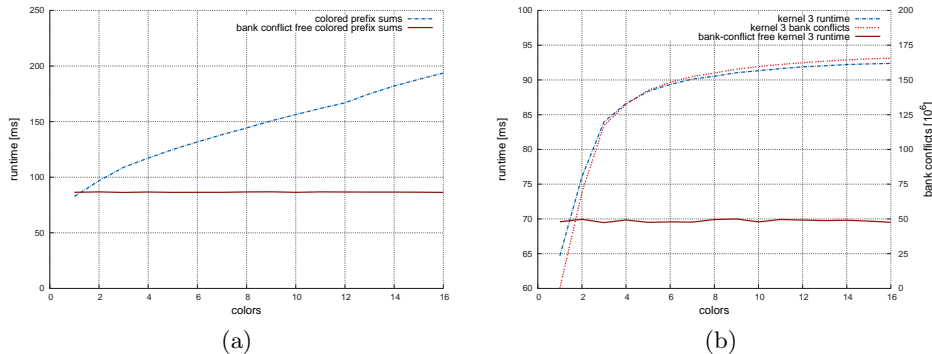


Fig. 1: The runtime of the colored prefix sums algorithm rises with increasing number of colors (a). The correlation between the number of bank conflicts and runtime can be seen in the example of the prefix sums kernel (b). The input size is 2^{29} elements (2 GB).

mergesort or bitonic mergesort). The likely reason for the success of sorting networks on GPUs is the small constant factors in the run time analysis of sorting networks and their data-oblivious nature. The data-obliviousness of sorting networks implies that the execution stream of every thread is the same regardless of the value of the input data. Thus, there is no need for conditional statements in the code which bodes well with the SIMD nature of threads in a warp.

However, the rigid access pattern of the sorting networks makes it difficult to avoid memory bank conflicts and over the decade of GPU computing no one has been able to come up with an efficient sorting network that causes no bank conflicts on inputs larger than the number of memory banks in shared memory.

1.4 Our Contributions

We present a framework for designing bank conflict free algorithms in shared memory. Using our framework we identified an existing 27 year old sorting algorithm as a candidate for a bank conflict free comparison-based sorting algorithm on GPUs for data as large as shared memory.

Using our new sorting algorithm as a subroutine, we developed a bank conflict free merging of pairs of sorted sequences, thus, producing *BCFMergesort* – the first fully bank conflicts free comparison-based sorting GPU algorithm.

The lack of bank conflicts in *BCFMergesort* allows us to perform a worst-case theoretical analysis and accurately predict the runtime of our algorithm on GPUs. This is the first comparison-based sorting algorithm on GPUs that we are aware of that has such theoretical analysis. We implemented our algorithm and show that it outperforms current GPU mergesort implementations.

Memory Bank 0	A_0	A_8	A_{16}	A_{24}	A_{32}	A_{40}	A_{48}	A_{56}										
Memory Bank 1	A_1	A_9	A_{17}	A_{25}	A_{33}	A_{41}	A_{49}	A_{57}										
Memory Bank 2	A_2	A_{10}	A_{18}	A_{26}	A_{34}	A_{42}	A_{50}	A_{58}										
Memory Bank 3	A_3	A_{11}	A_{19}	A_{27}	A_{35}	A_{43}	A_{51}	A_{59}										
Memory Bank 4	A_4	A_{12}	A_{20}	A_{28}	A_{36}	A_{44}	A_{52}	A_{60}										
Memory Bank 5	A_5	A_{13}	A_{21}	A_{29}	A_{37}	A_{45}	A_{53}	A_{61}										
Memory Bank 6	A_6	A_{14}	A_{22}	A_{30}	A_{38}	A_{46}	A_{54}	A_{62}										
Memory Bank 7	A_7	A_{15}	A_{23}	A_{31}	A_{39}	A_{47}	A_{55}	A_{63}										

Fig. 2: The view of shared memory as a $b \times \lceil M/b \rceil$ matrix.

2 Algorithmic Framework

Let P_h be the number of SMs on the hardware and M_h be the amount of shared memory available on each SM. Let P be the total number of CTAs. Let w be the number of threads within each warp and for simplicity we let w represent the number of banks in shared memory. Let M be the size of shared memory required by each CTA. We choose M to be at most $\frac{P_h \cdot M_h}{P}$ to guarantee that all CTAs can fit on all SMs and run concurrently without any context switches. Let W be the number of warps per CTA. We set P and W to be the minimum values which maximize the throughput between global and shared memories. For ease of exposition we define $p = PW$. In our experiments we observed that $p = PW = 8P_h$ was the optimal choice for P and W to maximize throughput. This relationship and the constraint $M \leq \frac{P_h \cdot M_h}{P}$ allows us to vary M depending on the specific needs of the algorithm.

During algorithm design, we treat $\Theta(M)$ elements as a single contiguous block and transfer these blocks between the global and shared memories. Note that $M > 32$, is the lower bound to perform such transfer in coalesced manner. Our experiments showed that loading $M \geq 1024$ elements per warp maximizes the throughput. Once M elements are in shared memory, we can focus on processing them without any bank conflicts as efficiently as possible.

2.1 Designing Bank Conflict Free Algorithms In Shared Memory

We extend the view of shared memory as observed by Dotsenko et al. [6]. Just like them we view the shared memory of size M as a matrix \mathcal{M} , with w rows and $\lceil \frac{M}{w} \rceil$ columns. Each row corresponds to one of the w memory banks. When r items are loaded into contiguous address space in shared memory, it is loaded in column major order into $\lceil \frac{r}{w} \rceil$ columns (see Figure 2). Dotsenko et al. used this view to pad the input to offset the starting indices of each thread, so that a parallel scan of contiguous data would result in each thread starting from a different memory bank.

We extend this view to computations other than parallel scan. In particular, observe that if we view the shared memory as a matrix and process it in such a way that each thread processes a separate row of the matrix, each thread will

be accessing a separate bank, thus resulting in no bank conflicts. Furthermore, observe that if we can transform the matrix from the column-major layout to the row-major layout without causing any bank conflicts, the original columns become rows and, therefore, the columns of the original matrix can also be processed without any bank conflicts.

A transformation of a square matrix between the two layouts is simply a transposition of it. A warp can perform bank conflict free transposition of a $w \times w$ matrix in $\frac{w}{2} - 1$ rounds, where in each round $i: 1 \leq i \leq \frac{w}{2} - 1$, each thread $0 \leq t \leq w - 1$ swaps the element $\mathcal{M}[t, (i+t) \bmod w]$ with the element $\mathcal{M}[(i+t) \bmod w, t]$. Note that within each reading or writing step, all w threads access a different row (memory bank) of the matrix. The lock-step execution among the threads of the warp ensures that the reads and writes are performed one after another without interfering with each other.

Since the transposition incurs no bank conflicts, all w threads can perform each step without interfering with each other and we can easily analyze the asymptotic worst-case runtime as $(\frac{w}{2} - 1) \cdot \mathcal{O}(1) = \mathcal{O}(w)$ parallel steps.

We can easily generalize the transformation for input sizes $n = hw^2$ for a small integer constant h that divides w . The details are presented in Appendix E.

3 BFCMergesort: Bank-conflict free sorting

For our bank conflict free sorting we chose the classic mergesort algorithm. Practical mergesort implementations distinguish two phases: the base case phase and the merging phase. In the base case phase, $\lceil \frac{N}{M} \rceil$ sequences of M elements each are sorted. The merging phase proceeds in $\lceil \log(\frac{N}{M}) \rceil$ rounds, in each round merging pairs of sorted sequences from the previous round to create increasingly larger sequences, until only a single sorted sequence remains. In this section, we present how to implement each of these phases without any bank conflicts.

3.1 Base case (ShearSort)

On GPUs, the base case is sorted in shared memory using a sorting network. Sorting networks are ideal for GPUs because they are data oblivious (resulting in no branch divergence) and they are very simple (resulting in very small constant factors). However, sorting networks still cause bank conflicts if the size of the sequence to be sorted is larger than w . This is probably the reason why the fastest mergesort implementations on GPUs (e.g. the Thrust library [15], the CUDPP library [5] and warpsort [18]) use sorting networks only for up to $2w = 64$ elements.

In 1983, Sen et al.[16] introduced ShearSort – a sorting network to sort numbers arranged in an $m \times m$ matrix in snake-like order along the column-major order. The algorithm proceeds in rounds. In each round it sorts even-numbered columns in ascending order and odd-numbered columns in descending order, then sorts each row in ascending order. Using 0-1 principle [8], it is easy to show that after $\Theta(\log m)$ rounds the matrix is sorted.

Using our observation from Section 2.1, it is easy to see that ShearSort can be implemented on GPUs to sort sequences of $M = w^2$ elements in shared memory with w banks without any bank conflicts. Using w threads, it will take $T_b(M) = \mathcal{O}(\hat{t}(\frac{M}{w}) \cdot \log w)$ parallel time, where $\hat{t}(n)$ is the time it takes to sort a row or a column of n elements using a single thread. We can still benefit from the simplicity and data-oblivious nature of traditional sorting networks by implementing sequential sorting of rows and columns with a sorting network. Thus, if the row/column sorting is implemented using Batcher’s sorting network [2], then $\hat{t}(n) = \mathcal{O}(n \log^2 n)$ and the total time it takes to sort $M = w^2$ elements is $T_b(M) = \mathcal{O}(\frac{M}{w} \log^3 w) = \mathcal{O}(w \log^3 w)$. Notice, that although this approach incurs $\mathcal{O}(\log w)$ extra steps over a simple implementation of a sorting network in shared memory, this time complexity is guaranteed in the worst case and our experiments show that the savings due to lack of bank conflicts are larger than the extra $\mathcal{O}(\log w)$ factor (see Section 4).

The following simple extension allows us to sort larger inputs: for any integer h that divides w , we can sort $M = w^2 h$ elements using h warps of a CTA. Remember that $w^2 h$ elements can be viewed in shared memory as a $w \times (wh)$ matrix. Each column of this matrix can be sorted as before. However, each row now consists of wh elements and sorting it using a single thread would be too slow. Instead, we first pack $\frac{w}{h}$ such rows into separate $w \times w$ matrices as follows. We transpose each of h square submatrices and gather the columns that comprise an original row of wh elements into adjacent columns. These columns can easily be identified using index arithmetic. Once each original row is packed into h contiguous columns, we run *Segmented ShearSort* on $w \times w$ submatrices. *Segmented ShearSort* is a modified ShearSort, which instead of sorting the whole rows of a square matrix, sorts groups of $\frac{w}{h}$ elements within each row. Thus, after $\log(\frac{w}{h})$ rounds, each $w \times (\frac{w}{h})$ submatrix corresponding to the original rows of wh elements will be sorted.

Transformation of the $w \times (wh)$ matrices takes $\mathcal{O}(w)$ parallel time when performed using h warps (wh threads). *Segmented ShearSort* of a square matrix using w threads takes $\mathcal{O}(\hat{t}(\frac{M}{wh}) \log \frac{w}{h}) = \mathcal{O}(w \cdot \log^2 w \cdot \log \frac{w}{h})$ parallel time, which is the total runtime for sorting $M = w^2 h$ elements using h warps.

3.2 Bank-conflict free merging

After sorting the base case, our algorithm performs a binary merge of the resulting sorted sequences using a separate warp to merge each pair of sequences.

Let P be the minimal number of CTAs that maximizes throughput, as mentioned in Section 2. If the number of sequences to be merged is fewer than $2P$, some of the CTAs will be sitting idle, thus, reducing the available parallelism. Ye et al. [18] presented a randomized approach to mitigate this problem. Their idea is to suspend binary merging when the number of sequences drops below $2P$, distribute the sequences into P buckets, such that all elements of bucket i are smaller than elements in bucket $i + 1$ for all buckets, and continue binary merging on the portions of the sequences within each bucket. Ye et al. choose bucket boundaries as random samples of the input. In this section we present a

deterministic approach for determining bucket boundaries, while adapting their merging algorithm to use our ShearSort from the previous section.

Binary merging. To merge two sorted sequences A and B , a standard sequential algorithm starts off by loading the smallest element from each sequence. Then it repeatedly outputs the smaller of the two items and loads the next element from the sequence, whose element was written out.

Since each warp consists of $w = 32$ threads, it is inefficient to load only one element from each sequence. Instead Ye et al [18] load a page of size $\frac{M}{2}$ from each sequence into shared memory, merge M elements using all w threads of a warp, output at least $\frac{M}{2}$ smallest elements, and load the next page of $\frac{M}{2}$ elements from the sequence, whose input is exhausted first.

In our implementation, we set $M = w^2$ and use our ShearSort implementation to merge the two pages in shared memory. Since both input sequences are already sorted, by the 0-1 principle we can reduce the number of rounds of ShearSort to just one, resulting in overall merging time $T_m(M) = \mathcal{O}\left(\hat{t}\left(\frac{M}{w}\right)\right) = \mathcal{O}(w \log^2 w)$.

Distribution. Each merge round reduces the number of sequences s by a factor of 2, causing the algorithm to terminate after $\mathcal{O}\left(\log\left(\frac{N}{M}\right)\right)$ rounds. However, if $s < 2P$, some CTAs will be idle while others have to work on longer sequences in each round. To improve resource utilization we suspend the merge at $s = P$ and distribute the sequences across P buckets. To determine the bucket boundaries deterministically, we adapt the approach of Aggarwal and Vitter [1].

Given s sorted sequences, each of size $\frac{N}{s}$, we pick t evenly spaced elements as potential splitters from each sequence and sort the st elements (let's call them S). We pick $P - 1$ evenly spaced items from S as the final splitters that define bucket boundaries. To perform the distribution of the s sequences into the P buckets defined by the $P - 1$ splitters, we calculate the rank of each splitter for every sorted sequence by parallel scans of the data, and sort the subsequences by bucket and sequence number.

Lemma 1. *Assuming all elements are distinct, the size of each bucket is at most $\mathcal{O}\left(\frac{N}{t} \cdot \left(1 + \frac{t}{P}\right)\right)$ elements.*

Proof. The number of elements within each sequence between any pair of potential splitters is $\lceil \frac{N}{st} \rceil$. There are $\lceil \frac{st}{P} \rceil$ potential splitters between a pair of selected final splitters. Thus, the total number of elements between final selected splitters is at most $s \cdot \lceil \frac{N}{st} \rceil + \lceil \frac{st}{P} \rceil \cdot \lceil \frac{N}{st} \rceil = \mathcal{O}\left(\frac{N}{t} \cdot \left(1 + \frac{t}{P}\right)\right)$.

Thus, if we pick $t = P$ potential splitters from each sequence, the size of each bucket is at most $\mathcal{O}\left(\frac{N}{P}\right)$.

Final merge phase. After rearranging the data the number of sorted subsequences is P^2 . CTA p_i then sorts the i th bucket by merging the sorted subsequences of the bucket. Since the subsequences may have sizes that are not a multiple of the page size, padding is introduced implicitly in shared memory, but not written to the output array.

This phase requires $\log(P)$ additional merge rounds in which none of the P CTAs runs out of work prematurely.

Lemma 2. *BCFMergesort takes $\mathcal{O}\left(\frac{N}{Pw} \cdot (1 + \log^2(w) \cdot \log\left(\frac{N}{w}\right))\right)$ time and requires $\mathcal{O}\left(1 + \log\left(\frac{N}{M}\right)\right)$ parallel scans of the data in global memory.*

Proof. The proof for Lemma 2 can be found in Appendix B.

3.3 Optimizations

Use of registers. While latency of accessing shared memory is much lower than accessing global memory, it still incurs some latency. Any computation that requires multiple accesses to the same location in shared memory can be sped up by implementing it in registers. Since our GPU hardware has 64 physical registers per thread (63 of which can be used for data), and our ShearSort sorts $M = w^2$ elements, where $w = 32$, the sorting of each row (and column after the matrix transposition) of the $w \times w$ matrix can be implemented in registers. Note that the indices for accessing registers when loading a row of $w = 32$ elements do not depend on the thread index and the data is not transferred to local memory. The effects of register optimization are presented in Appendix D.

Implicit matrix transposition. Processing the columns of the $w \times w$ matrix requires transposition of the matrix. The challenge with loading the column directly into registers is the fact that it either causes bank conflicts, or the indices of registers being loaded must depend on the thread identifier. The latter case causes the local memory (instead of actual registers) being used, which is actually implemented in off-chip global memory (see Section 1.1). Thus, neither of the approaches is acceptable. However, if we define column j as *shifted diagonals* of the matrix (i.e. matrix elements $\mathcal{M}[(j+k) \bmod w, k]$ for $0 \leq k < w$) and row i to be the i th column, shifted upwards by i elements (i.e. elements $\mathcal{M}[(i+k) \bmod w, i]$ for $0 \leq k < w$), we can load each row and column directly into registers without the need for transposition.

Duplicate keys. Lemma 1 guarantees that bucket sizes are at most a constant factor more than $\frac{N}{P}$ only if all the items are distinct. A large number of duplicates might cause some bucket to be much larger than others. To mitigate this issue, we define additional $P - 1$ buckets and place all items equal to the bucket boundary into their own bucket. Thus, after the distribution, any duplicate items equal to bucket boundaries will already be in the correct position and do not need to be processed any further. We call this version *BCFMergesortPB*.

4 Experimental results

We conduct our experiments on a standard PC with a 2.4 GHz Intel Core2 Quad CPU, 8 GB of RAM and an NVIDIA Geforce GTX580 GPU with 3 GB of memory, $P_h = 16$ SMs and $M_h = 48$ KB per SM (with additional 16KB used for caching local memory). There are $w = 32$ physical cores per SM, $w = 32$ threads per warp and the shared memory consists of $w = 32$ banks. Our algorithms are implemented using the CUDA runtime API and compiled with the CUDA toolkit version 5.5, gcc version 4.7 and the `-O 3` optimization flag. The runtimes

reported do not include the time needed to transfer data from the host computer to the GPU or back.

We compare our sorting algorithm to the well-known implementation of the Thrust library [3] (version 1.7) and warpsort [18].³ We did not include CUDPP mergesort [5] in our experiments, as the available code imposes severe limitations on the input and does not sort data larger than 64 MB. Unfortunately, we also couldn't find a working implementation of the Samplesort [9] for our hardware.

We report performance on four different data sets: *Random* data set consists of keys chosen uniformly from $[0 \dots 10^6]$, *distinct* data set is the sequence $1 \dots n$ permuted by a shuffle algorithm [7], *0-1* data set contains uniformly chosen entries of zero or one and *defined duplicates* data set is formed by k copies of each of $\frac{n}{k}$ distinct keys, randomly permuted by the shuffle algorithm.

Warpsort uses a bucket distribution as well, but the splitter selection is randomized. It is known that deterministic algorithms result in significantly slower implementations in practice. Therefore, it is notable that our deterministic algorithms are only slightly slower than the randomized warpsort.

Duplicate keys skew the bucket sizes of the BCFMergesort. The effects of having separate buckets for pivot values can be seen in Figure 4. It's notable that warpsort fails to sort *0-1* data completely.

Though our merge algorithm is not in-place either, it requires less extra space than both Thrust and warpsort. BCFMergesort lets us sort up to 1GiB of data on our hardware, while Thrust and warpsort run on inputs up to 512 MiB and 256MiB, respectively.

The relevant parameters for the merge phase were empirically determined to be $p = 8P_h = 128$ and $M = w^2 = 1024$.

The runtimes per key for the different algorithms and different input sets are shown in Figures 3 and 4. BCFMergesort with pivot buckets (BCFMergesortPB) for inputs with few distinct keys suffers a performance loss of 6% compared to our normal mergesort. While warpsort falls exactly into this gap for random keys, the randomized pivot selection appears to be beneficial when dealing with inputs with all distinct keys, putting it on par and even surpassing our normal mergesort on two instances. And while thrust mergesort is slightly faster than BCFMergesort on the smallest instance (5%), we beat thrust by up to 64% on *random* inputs and 54% on *distinct* keys.

The chart for *0-1* data impressively shows the strength of pivot buckets introduced at the end of Section 3.2. Since the heuristic causes BCFMergesortPB to have nothing more to do after rearranging the data, BCFMergesortPB beats BCFMergesort on these inputs by a factor of up to 15.5 and thrust sort by a factor of up to 2.7. In the chart for *defined duplicates*, the less extreme versions

³ The results for warpsort presented in [18] included heuristics not mentioned in the paper. Unfortunately, these heuristics did not guarantee the runtimes mentioned in the paper and because of this the warpsort would run much slower for some inputs. Therefore, (with the approval of the authors of [18]) we modified warpsort to align with the description within their paper, resulting in more uniform runtimes, albeit slightly slower than what is presented in [18].

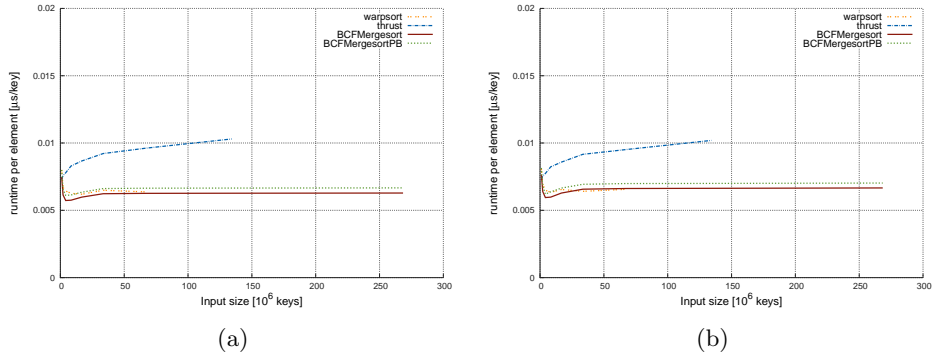


Fig. 3: Runtime per key for the *random* (a) and *distinct* (b) data sets.

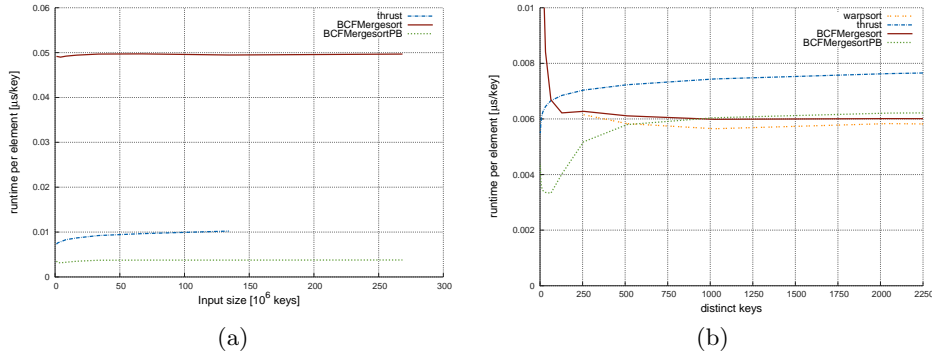


Fig. 4: Runtime per key for the *0-1* (a) and *defined duplicates* (b) data sets. For *defined duplicates* we limit the axes to display the interesting part. BCFMergesort for two distinct keys takes $0.051 \mu\text{s}$ per key. Input size for (b) is 2^{25} keys.

of up to 2250 distinct keys can be seen. BCFMergesortPB first surpasses the normal version of BCFMergesort when $\frac{1}{4}$ of all keys are equal to a splitter.

5 Conclusion

We discussed the properties of GPUs, focusing on the memory hierarchy. We provide experimental data that shows the great impact of shared memory bank conflicts on the runtime of GPU programs and described methods to design bank conflict free algorithms for GPUs. Using those methods, we developed the first comparison-based bank conflict free sorting algorithm for GPUs and showed that the benefits of having no bank conflicts outweigh the additional work necessary to make algorithms bank conflict free.

Acknowledgments. We would like to thank Vitaly Osipov for helpful discussions and sharing his insights on GPUs.

References

1. Aggarwal, A., Vitter, J.: The Input/Output Complexity of Sorting and Related Problems. *Communications of the ACM* pp. 1116–1127 (1988)
2. Batcher, K.E.: Sorting Networks and their Applications. In: *Proceedings of the AFIPS Spring Joint Computer Conference*. pp. 307–314. ACM (1968)
3. Bell, N., Hoberock, J.: Thrust: A productivity-oriented library for CUDA. *GPU Computing Gems: Jade Edition* pp. 359–372 (2011)
4. Cederman, D., Tsigas, P.: A Practical Quicksort Algorithm for Graphics Processors. In: *Algorithms-ESA 2008*, pp. 246–258. Springer (2008)
5. Davidson, A., Tarjan, D., Garland, M., Owens, J.D.: Efficient Parallel Merge Sort for Fixed and Variable Length Keys. In: *Innovative Parallel Computing (InPar), 2012*. pp. 1–9. IEEE (2012)
6. Dotsenko, Y., Govindaraju, N.K., Sloan, P.P., Boyd, C., Manfredelli, J.: Fast Scan Algorithms on Graphics Processors. In: *Proceedings of the 22nd Annual International Conference on Supercomputing* (2008)
7. Knuth, D.E.: *Seminumerical Algorithms, The Art of Computer Programming*, vol. 2. Addison-Wesley, Reading, third edn. (1998)
8. Knuth, D.E.: *Sorting and Searching, The Art of Computer Programming*, vol. 3. Addison-Wesley, Reading, third edn. (1998)
9. Leischner, N., Osipov, V., Sanders, P.: GPU Sample Sort. In: *Proceedings of the 24th IEEE Parallel and Distributed Processing Symposium (IPDPS)* (2010)
10. Merrill, D., Grimshaw, A.: Parallel Scan for Stream Architectures. Tech. Rep. CS2009-14, Department of Computer Science, University of Virginia (2009)
11. Merrill, D., Grimshaw, A.: High Performance and Scalable Radix Sorting: A Case Study of Implementing Dynamic Parallelism for GPU Computing. *Parallel Processing Letters* 21(02), 245–272 (2011)
12. NVIDIA: *NVIDIA CUDA Programming Guide 5.0* (2012), http://docs.nvidia.com/cuda/pdf/CUDA_C_Programming_Guide.pdf, last viewed on 2/11/2013
13. Peters, H., Schulz-Hildebrandt, O., Luttenberger, N.: Fast In-Place Sorting with CUDA based on Bitonic Sort. In: *Parallel Processing and Applied Mathematics*, pp. 403–410. Springer (2010)
14. Purcell, T.J., Donner, C., Cammarano, M., Jensen, H.W., Hanrahan, P.: Photon Mapping on Programmable Graphics Hardware. In: *Proceedings of the ACM SIGGRAPH/EUROGRAPHICS conference on Graphics hardware*. pp. 41–50. Eurographics Association (2003)
15. Satish, N., Harris, M., Garland, M.: Designing Efficient Sorting Algorithms for Manycore GPUs. In: *Proceedings of the 23rd IEEE Parallel and Distributed Processing Symposium (IPDPS)*. pp. 1–10. IEEE (2009)
16. Sen, S., Scherson, I.D., Shamir, A.: Shear Sort: A True Two-Dimensional Sorting Techniques for VLSI Networks. In: *ICPP*. pp. 903–908 (1986)
17. Sintorn, E., Assarsson, U.: Fast Parallel GPU-Sorting using a Hybrid Algorithm. *Journal of Parallel and Distributed Computing* 68(10), 1381–1388 (2008)
18. Ye, X., Fan, D., Lin, W., Yuan, N., Jenne, P.: High Performance Comparison-Based Sorting Algorithm on Many-Core GPUs. In: *Proceedings of the 24th IEEE Parallel and Distributed Processing Symposium (IPDPS)* (2010)

A Impact of Bank Conflicts on Runtimes

The importance of shared memory bank conflicts can easily be demonstrated by looking at the problem of *colored prefix sums*: given an array of N elements and a set of d colors $\{c_1, c_2, \dots, c_d\}$, with a color c_i associated with each element, colored prefix sums asks to compute d independent prefix sums among the elements of the same color.

Our algorithm is basically a three-phase prefix sums algorithm similar to Merrill’s [10]. The elements are assigned to P CTAs in contiguous tiles of size $\frac{N}{P}$. For colored prefix sums, we keep intermediate values for each color and perform extra operations to identify the color of each element.

In the first phase all elements of the tiles are reduced using the prefix sums operation. This results in d values per CTA, one for each color. The second phase calculates the prefix sums of those $P \cdot d$ reduced values as offsets for the neighboring tiles. This can be done on a single CTA interpreting the values as a $d \times P$ matrix. In the final phase, the prefix sums of the tiles are calculated, seeded with the offsets computed in the second phase. Since the tiles may be too large for shared memory, they are loaded in contiguous pages of M elements. Between neighboring pages, page offsets for each color have to be stored in shared memory. The calculation of colored prefix sums within a page resembles the algorithm itself: Each thread is assigned a contiguous chunk of the page and first counts the entries per color in its chunk, then the intra-page offsets are calculated by one scan of those sums per color, and finally the threads calculate colored prefix sums on their chunks seeded with the tile-, inter-page and intra-page offsets.

We would expect the runtime to depend on the input size N , the number of CTAs P and the warp size w , but not d since all calculations depending on the number of colors are performed in parallel. However, the runtime increases with the number of colors (see Figure 1). The slowdown correlates nicely with the number of shared memory bank conflicts incurred when calculating intra-page offsets in the third phase.

To improve our algorithm, we implement a way to calculate the intra-page offsets without any bank conflicts. We assign each thread one memory bank for storage of intermediate values. The resulting $w \times d$ matrix lists the color values in columns. To avoid having multiple threads working on the same banks we transpose the matrix and then calculate the prefix sums with d threads in parallel. After retransposing the matrix, we can propagate the offsets.

We observe that the runtime of the algorithm is now constant for different numbers of colors (see Figure 1). We limit the number of colors to 16 because of the limited amount of shared memory available for each multiprocessor.

B Proof for Lemma 2

Proof. The BCFMergesort runs in four basic phases: the base case phase, the first merge phase, the bucket distribution and the final merge phase. We will look at each phase separately and combine the results later.

The base case phase uses P CTAs working in parallel to sort the input in $\frac{N}{M}$ segments of size M . Each CTA has to perform $\lceil \frac{N}{M \cdot P} \rceil$ rounds of sorting, resulting in $\mathcal{O}\left(\frac{N}{M \cdot P} \cdot \hat{t}(w) \cdot \log(w)\right)$ parallel time. In the process, each data item is read and written once.

To reduce the number of sorted sequences to P , $\log\left(\frac{N}{M \cdot P}\right)$ rounds of binary merge have to be performed in the first merge phase. To merge two sequences of size $\frac{N}{2}$, a total of $2 \cdot \frac{N/2}{M/2} = \frac{2 \cdot N}{M}$ pages of size $\frac{M}{2}$ have to be processed in each round: one page is read, two pages are merged, one page is written. Therefore, each element is merged twice in average, resulting in a parallel time of $\mathcal{O}\left(\frac{N}{M \cdot P} \cdot \log\left(\frac{N}{M \cdot P}\right) \cdot \hat{t}(w)\right)$ and $\log\left(\frac{N}{M \cdot P}\right)$ additional reads and writes of the data.

The bucket distribution in itself consists of five phases: picking t pivots from each sorted sequence, sorting those $t \cdot P$ pivots, choosing the $P - 1$ final pivots and finding their location in the sorted sequences, calculating the splitter offsets and rearranging the data by bucket. Since we use one CTA per sorted sequence, selecting t pivots takes $\mathcal{O}\left(\frac{t}{w}\right)$ time.

The pivots are then sorted using mergesort: base case and binary merge phases. That results in $\mathcal{O}\left(\frac{P^2}{M} \cdot \hat{t}(w) \cdot \log(w) + \log\left(\frac{P^2}{M}\right) \cdot \hat{t}(w)\right) = \mathcal{O}\left(\frac{P^2}{M} \cdot \hat{t}(w) \cdot \log(w)\right)$ parallel time.

The splitter are located by sequentially scanning the sequences using w threads for each. Therefore, each CTA needs $\mathcal{O}\left(\frac{N}{Pw}\right)$ time. In the process, the data is read once.

The calculation of the P^2 subsequence offsets takes another $\mathcal{O}(P)$ time.

Finally, the data is rearranged. Each of the P CTAs moves P subsequences to their proper positions, causing $\mathcal{O}(P)$ computation and one more read and write of all data.

The final merge phase causes another $\log(P)$ binary merges. Implicit padding can at most be $\frac{M}{2} - 1$ elements per subsequence, $\left(\frac{M}{2} - 1\right) \cdot P^2$ in total. This is $\mathcal{O}(N)$ for any reasonable combination of parameters, so the time of the page-wise binary merge applies.

This results in a total parallel runtime of

$$\begin{aligned}
& \mathcal{O}\left(\frac{N}{M \cdot P} \cdot \hat{t}(w) \cdot \log(w)\right) + \mathcal{O}\left(\frac{N}{M \cdot P} \cdot \log\left(\frac{N}{M \cdot P}\right) \cdot \hat{t}(w)\right) \\
& + \mathcal{O}\left(\frac{t}{w}\right) + \mathcal{O}\left(\frac{P^2}{M} \cdot \hat{t}(w) \cdot \log(w)\right) + \mathcal{O}\left(\frac{N}{Pw}\right) + \mathcal{O}(P) + \mathcal{O}(P) \\
& + \mathcal{O}\left(\frac{N}{M \cdot P} \cdot \log(P) \cdot \hat{t}(w)\right) \\
& = \mathcal{O}\left(\frac{N}{M \cdot P} \cdot \hat{t}(w) \cdot \log(w) + \frac{N}{M \cdot P} \cdot \log\left(\frac{N}{M \cdot P}\right) \cdot \hat{t}(w) + \frac{N}{Pw} + \frac{N}{M \cdot P} \cdot \log(P) \cdot \hat{t}(w)\right) \\
& = \mathcal{O}\left(\frac{N}{M \cdot P} \cdot \hat{t}(w) \cdot \left(\log(w) + \log\left(\frac{N}{M \cdot P}\right) + \log(P)\right) + \frac{N}{Pw}\right) \\
& = \mathcal{O}\left(\frac{N}{M \cdot P} \cdot \hat{t}(w) \cdot \log\left(\frac{N \cdot w}{M}\right) + \frac{N}{Pw}\right).
\end{aligned}$$

Considering that $M = w^2$ and $\hat{t}(w) = w \cdot \log^2(w)$, we get

$$\begin{aligned}
& \mathcal{O}\left(\frac{N}{M \cdot P} \cdot \hat{t}(w) \cdot \log\left(\frac{N \cdot w}{M}\right) + \frac{N}{Pw}\right) \\
& = \mathcal{O}\left(\frac{N}{Pw} \cdot \log^2(w) \cdot \log\left(\frac{N}{w}\right) + \frac{N}{Pw}\right) \\
& = \mathcal{O}\left(\frac{N}{Pw} \cdot \left(1 + \log^2(w) \cdot \log\left(\frac{N}{w}\right)\right)\right).
\end{aligned}$$

and in $\mathcal{O}\left(1 + \log\left(\frac{N}{M \cdot P}\right) + \log(P)\right) = \mathcal{O}\left(1 + \log\left(\frac{N}{M}\right)\right)$ passes over the data.

C Additional charts

For completeness we present the plain runtime charts of GPU mergesort algorithms in Figures 5 and 6. The dominance of the linear term makes it difficult to see the lower order terms, for sorting, which is the reason why we chose to normalize the runtimes per element in the main presentation of the results.

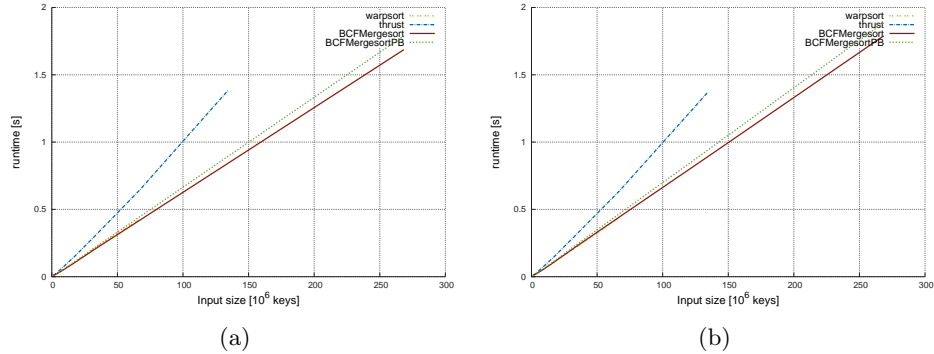


Fig. 5: Runtime for the *random* (a) and *distinct* (b) data sets.

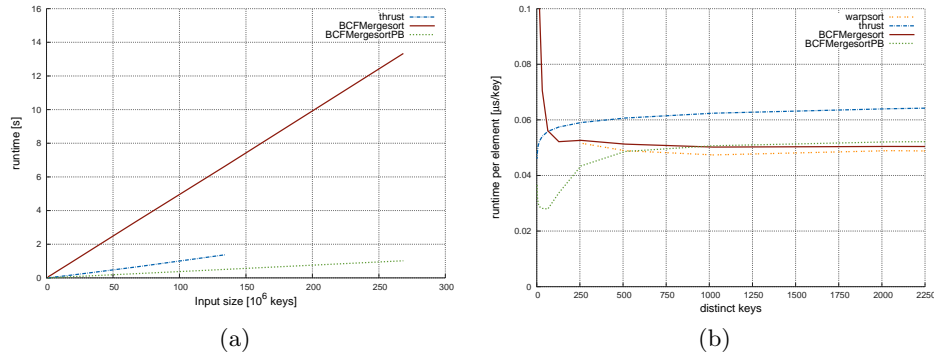


Fig. 6: Runtimes for the *0-1* (a) and *defined duplicates* (b) data sets. For *defined duplicates* we limit the axes to display the interesting part. BCFMergesort for two distinct keys takes $0.051 \mu s$ per key. Input size for (b) is 2^{25} keys.

D Register optimization

We ran experiments to determine the speedup provided by sorting rows and columns in register space. The results in Figure 7 show the runtimes of BCFMergesort with transposition on a $w \times w$ matrix with register optimization and without. As a comparison, we also provide the runtime of an implementation of Odd-Even Transposition Sort on $w^2 = 1024$ elements. It demonstrates the effect of bank conflicts in shared memory on runtimes. The sorting algorithms are applied to subsets of w^2 elements on the total input of 2^{25} elements.

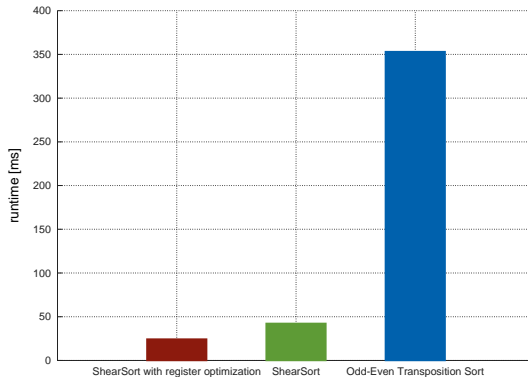


Fig. 7: Comparison of runtimes of ShearSort with and without register optimization and of Odd-Even Transposition sorting network on subsets of 1024 elements each, for the total of size of 2^{25} elements.

E Bank-conflict free computation on non-square matrices

The approach to bank conflict free computation from Section 2.1 can easily be generalized for inputs of size $n = hw^2$ for a small integer constant h that divides w , by transforming the input from column-major to row-major order and vice versa. Since space in shared memory is limited [12], it is desirable to perform this transformation in-place. Although there is no simple in-place algorithm for transforming general rectangular matrices from row-major to column-major order, h is a sufficiently small integer for current sizes of shared memories on GPUs (currently $h \leq 12$).

To transform the matrix from column-major to row-major layout, we split the $w \times hw$ matrix into h square $w \times w$ matrices, transpose each one using a different warp (see Figure 8), and combine h original columns (now h partial rows) that compose a single hw -sized row using all h warps (see Figure 9). Transformation from row-major to column-major layout is done similarly. For pseudocode refer to Appendix F.

Then all h columns resulting from the transformation of the same row are gathered together in the correct order. The gathering of all h columns resulting from the transformation of the same row can be done by $h \cdot w$ threads in parallel without bank conflicts, because the w threads of the same warp will always run in lock-step. Each thread is responsible for one element of each resulting column of $\frac{w}{h}$ rows.

When analyzing the runtime of transforming a $w \times hw$ matrix one might think that running h warps on the same streaming multiprocessor with only w physical cores would increase the runtime by a factor of h . However, in practice

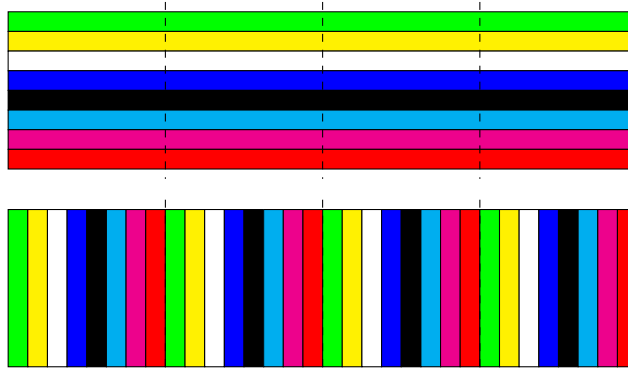


Fig. 8: 8×32 matrix with division into 8×8 -submatrices, before and after transforming the square submatrices

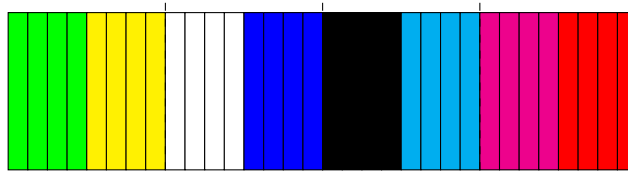


Fig. 9: The columns resulting from each row are gathered and placed in ascending order of rows.

this is not the case. The reason is that as long as all data required by the warps fits in the shared memory the context switch across the warps incurs no overhead and running a single warp takes the same time as running h warps with extra time spent waiting for data access due to the latency of accessing shared memory.

Since there are no bank conflicts in this procedure, the runtime of transforming an $w \times hw$ matrix remains $\mathcal{O}(w)$ time.

F Pseudocode of BCFMergesort

Sorting w^2 elements in shared memory without bank conflicts. ShearSort sorts a matrix of values in snake-like order by first sorting the rows in alternating directions and then columns in ascending order. We use the fact that transforming a square matrix in shared memory from column-major to row-major order can be done by simply transposing the matrix (see Algorithm 1). That way our implementation can assign one memory bank to each of the w threads (see Section 3.1). For simplicity we assume that the result should be sorted in ascending order. Since all threads execute the same program in parallel, this pseudocode is written for one thread with index tid .

Algorithm 1 SHEARSORT: Bank-conflict free sorting in shared memory

INPUT: $w \times w$ matrix m
OUTPUT: Sorted matrix m

register array $R[w]$
FOR i IN $1 \dots \log_2(w)$ DO
 # Sort the rows of matrix m in alternating order
 FOR j in $0 \dots (w - 1)$ DO $R[j] = m[tid][j]$

 BATCHERS-ODD-EVEN-MERGESORT(R)

 IF $tid \bmod 2 == 0$ THEN
 FOR j in $0 \dots (w - 1)$ DO $m[tid][j] = R[j]$
 ELSE
 FOR j in $0 \dots (w - 1)$ DO $m[tid][w - j] = R[j]$

 # Change matrix from column-major order to row-major order
 TRANSPOSE(m)

 # Sort the columns of matrix m
 FOR j in $0 \dots (w - 1)$ DO $R[j] = m[tid][j]$

 BATCHERS-ODD-EVEN-MERGESORT(R)

 FOR j in $0 \dots (w - 1)$ DO $m[tid][j] = R[j]$

 # Change matrix from row-major order to column-major order
 TRANSPOSE(m)

 # Clean up and remove snake-like order
 FOR j in $0 \dots (w - 1)$ DO $R[j] = m[tid][j]$

 BATCHERS-ODD-EVEN-MERGESORT(R)

 FOR j in $0 \dots (w - 1)$ DO $m[tid][j] = R[j]$

 # Change matrix from column-major order to row-major order
 TRANSPOSE(m)

As explained in Section 3.3, the transpositions can be removed if we treat diagonals as columns and shifted columns as rows. The pseudocode for this optimization can be seen in Algorithm 2. The extra step of transforming diagonals to rows at the end of the algorithm is easily amortized by the missing $2 \cdot \log_2(w) + 1$ transpositions.

Algorithm 2 SHEARSORT-DIAGONAL: Bank-conflict free sorting in shared memory without transpositions

```

INPUT:  $w \times w$  matrix  $m$ 
OUTPUT: Sorted matrix  $m$ 

register array  $R[w]$ 
FOR  $i$  IN  $1 \dots \log_2(w)$  DO
  # Sort the diagonals of matrix  $m$  in alternating order
  FOR  $j$  IN  $0 \dots (w - 1)$  DO  $R[j] = m[(tid + j) \bmod w][j]$ 

  BATCHERS-ODD-EVEN-MERGESORT( $R$ )

  IF  $tid \bmod 2 == 0$  THEN
    FOR  $j$  IN  $0 \dots (w - 1)$  DO  $m[(tid + j) \bmod w][j] = R[j]$ 
  ELSE
    FOR  $j$  IN  $0 \dots (w - 1)$  DO  $m[(tid + w - j) \bmod w][w - j] = R[j]$ 

  # Sort the shifted columns of matrix  $m$ 
  FOR  $j$  IN  $0 \dots (w - 1)$  DO  $R[j] = m[(tid + j) \bmod w][tid]$ 

  BATCHERS-ODD-EVEN-MERGESORT( $R$ )

  FOR  $j$  IN  $0 \dots (w - 1)$  DO  $m[(tid + j) \bmod w][tid] = R[j]$ 

# Remove snake-like order
FOR  $j$  IN  $0 \dots (w - 1)$  DO  $R[j] = m[(tid + j) \bmod w][j]$ 

BATCHERS-ODD-EVEN-MERGESORT( $R$ )

FOR  $j$  IN  $0 \dots (w - 1)$  DO  $m[(tid + j) \bmod w][j] = R[j]$ 

# Transform diagonals to columns
FOR  $j$  IN  $0 \dots (w - 1)$  DO  $R[j] = m[(2 \cdot tid + j) \bmod w][(j + tid) \bmod w]$ 
FOR  $j$  IN  $0 \dots (w - 1)$  DO  $m[(tid + j) \bmod w][tid] = R[j]$ 

```

Sorting $h \cdot w^2$ elements in shared memory without bank conflicts. We extend our ShearSort implementation to matrices of size $w \times (h \cdot w)$. We define the functions CHANGE-TO-ROWMAJOR (Algorithm 3) and CHANGE-TO-COLUMNMAJOR (Algorithm 4) that transforms the long rows into h columns of size w . These functions require h warps.

Furthermore, SHEARSORT has to be modified to handle the long rows (Algorithm 5). For this procedure to run, we need a subroutine SHEARSORT-SEGMENTED

Algorithm 3 CHANGE-TO-ROWMAJOR: Turn column-major long matrices to row-major order

INPUT: $w \times (wh)$ matrix m
OUTPUT: Transformed matrix m

$widx = \lfloor \frac{tid}{w} \rfloor$
 $wpos = tid \bmod w$

Change all $w \times w$ submatrices $m_1 \dots m_h$ of matrix m to row-major order
TRANSPPOSE(m_{widx})

register array $R[w]$
FOR i in $0 \dots (\frac{w}{h} - 1)$ DO
 FOR j in $0 \dots (h - 1)$ DO
 $R[h \cdot i + j] = m[wpos][widx \cdot \frac{w}{h} + i] + j \cdot w$

FOR i in $0 \dots (w - 1)$ DO
 $m[wpos][widx \cdot w + i] = R[i]$

Algorithm 4 CHANGE-TO-COLUMNMAJOR: Turn row-major long matrices to column-major order

INPUT: $w \times (wh)$ matrix m
OUTPUT: Transformed matrix m

$widx = \lfloor \frac{tid}{w} \rfloor$
 $wpos = tid \bmod w$

register array $R[w]$
FOR i in $0 \dots (w - 1)$ DO
 $R[i] = m[wpos][widx \cdot w + i]$

FOR i in $0 \dots (\frac{w}{h} - 1)$ DO
 FOR j in $0 \dots (h - 1)$ DO
 $m[wpos][widx \cdot \frac{w}{h} + i] + j \cdot w = R[h \cdot i + j]$

Change all $w \times w$ submatrices $m_1 \dots m_h$ of matrix m to row-major order
TRANSPPOSE(m_{widx})

that takes three parameters: the matrix, the number of rows per segment and a flag snake-like that indicates whether the segments should be rearranged in the snake-like order required by ShearSort. `SHEARSORT-SEGMENTED` performs `SHEARSORT` where the second sort (the columns) is replaced by a *segmented sort* routine that sorts $\frac{w}{h}$ segments of size h .

For the diagonal version of `BCFMergesort`, changing the matrix to a different memory representation is reduced to gathering and scattering the diagonals in the same manner as `CHANGE-TO-ROWMAJOR` or `CHANGE-TO-COLUMNMAJOR` treat the columns.

Page-wise binary merge. To perform the bank conflict free page-wise binary merge (see Section 3.2), we load one page of data from both input streams, merge them and output one full page. Figuratively, the keys from the first exhausted page are moved to the other stream and are replaced keys from that stream. That is why merging has to continue until both streams are exhausted and cannot be stopped when the first input stream is finished.

For a better performance we modify the `SHEARSORT` subroutine to only perform one round of ShearSort instead of $\log_2(w)$. By the 0-1 principle this is enough to merge two sorted sequences. We call this shortened sorting routine `SHEARSORT-MERGE(S)`.

In the case of arbitrary input stream sizes, we have to determine the amount of data to load (e.g. by setting an integer $ls = \min(\frac{M}{2}, n[e] - ic[e])$) and in case of partially filled pages pad them with ∞ . Since the padding will remain in shared memory until the merge is finished, we also have to keep track of the amount of padding used and subtract it from the size of the final outputs.

Bucket distribution. The bucket distribution of Section 3.2 consists of two phases: finding the splitters and determining their positions in the input data, and rearranging the data. The second part is not strictly necessary but it makes life easier when the merging begins again.

The subroutine `FIND-BUCKETS` is called on P CTAs, identified by their index pid , with w threads each. The sorted substreams of input stream I are marked as $I_1 \dots I_P$. We also need a function `EXCLUSIVE-PREFIX-SUMS` that performs the namesake operation on P integers. Since $P = 128$ in our experiments, we chose a simple linear solution executed on one thread.

Algorithm 5 SHEARSORT-LONG: Bank-conflict free sorting of long matrices
in shared memory

INPUT: $w \times (wh)$ matrix m
OUTPUT: Sorted matrix m

```
register array  $R[w]$ 
FOR  $i$  IN  $1 \dots \log_2(w)$  DO
  # Change matrix to row-major order
  CHANGE-TO-ROWMAJOR( $m$ )

  # Change all segmented  $w \times w$  submatrices  $m_1^s \dots m_h^s$  from row-major order to column-major order
  TRANSPOSE( $m_{widx}^s$ )

  # Segmented sort submatrices  $m_1^s \dots m_h^s$  of matrix  $m$  in snake-like order
  SHEARSORT-SEGMENTED( $m_{widx}, h, \text{true}$ )

  # Change matrix to column-major order
  CHANGE-TO-COLUMNMAJOR( $m$ )

  # Change submatrices  $m_1 \dots m_h$  from column-major order to row-major order
  TRANSPOSE( $m_{widx}$ )

  # Sort the columns of all submatrices  $m_1 \dots m_h$ 
  FOR  $j$  in  $0 \dots (w - 1)$  DO  $R[j] = m_{widx}[tid][j]$ 
  BATCHERS-ODD-EVEN-MERGESORT( $R$ )
  FOR  $j$  in  $0 \dots (w - 1)$  DO  $m_{widx}[tid][j] = R[j]$ 

  # Change submatrices  $m_1 \dots m_h$  from row-major order to column-major order
  TRANSPOSE( $m_{widx}$ )

# Change matrix to row-major order
CHANGE-TO-ROWMAJOR( $m$ )

# Change segmented submatrices  $m_1^s \dots m_h^s$  from row-major order to column-major order
TRANSPOSE( $m_{widx}^s$ )

# Segmented sort submatrices  $m_1^s \dots m_h^s$  in ascending order
SHEARSORT-SEGMENTED( $m_{widx}, h, \text{false}$ )
```

Algorithm 6 BINARY-MERGE: Page-wise binary merge

INPUT: Streams $I[0]$ and $I[1]$, stream size n
OUTPUT: Output stream O

shared memory array $S[M]$
integer e

Load a page of $\frac{M}{2}$ keys from each input stream into S
 $S[0 \dots (\frac{M}{2} - 1)] = I[0][0 \dots (\frac{M}{2} - 1)]$
 $S[\frac{M}{2} \dots (M - 1)] = I[1][0 \dots (\frac{M}{2} - 1)]$

Determine the input stream, whose page will be exhausted first
IF $S[\frac{M}{2} - 1] \leq S[M - 1]$ THEN
 $e = 0$
ELSE
 $e = 1$

Merge the first pages of both input streams
SHEARSORT-MERGE(S)

Write the first page to the output stream
 $O[0 \dots (\frac{M}{2} - 1)] = S[0 \dots (\frac{M}{2} - 1)]$

Offset counters for all streams
integer $ic[0] = ic[1] = oc = \frac{M}{2}$

WHILE ($ic[0] < n$) OR ($ic[1] < n$) DO
 # If there are elements left in the designated input stream, load a page.
 # Otherwise load a page from the other stream. Adjust the offset counter.
 IF $ic[e] \geq n$ THEN $e = 1 - e$
 $S[0 \dots (\frac{M}{2} - 1)] = I[e][ic[e] \dots (ic[e] + \frac{M}{2} - 1)]$
 $ic[e] = ic[e] + \frac{M}{2}$

Determine which is the next page to be exhausted
IF $S[\frac{M}{2} - 1] > S[M - 1]$ THEN $e = 1 - e$

Merge the pages in shared memory
SHEARSORT-MERGE(S)

Write the next page to the output stream and adjust the offset counter
 $O[oc \dots (oc + \frac{M}{2} - 1)] = S[0 \dots (\frac{M}{2} - 1)]$
 $oc = oc + \frac{M}{2}$

Write the final remaining page to the output stream
 $O[oc \dots (2 \cdot n - 1)] = S[\frac{M}{2} \dots (M - 1)]$

Algorithm 7 FIND-BUCKETS: Bucket distribution

INPUT: Input stream I , consisting of P sorted substreams of size n , number of pivots t
OUTPUT: Output stream O , stream separators Q

```
global potential pivot array  $S[P \cdot t]$ 
global final pivot array  $F[P]$ 
global temporary splitter array  $T[P^2]$ 
global bucket offset array  $B[P]$ 
integer  $c, oc$ 

# Pick  $t$  potential splitters per substream  $I_k$ 
FOR  $i$  in  $0 \dots t$  DO  $S[pid \cdot t + i] = I_{pid}[i \cdot \frac{n}{t}]$ 

# Sort all potential pivots
MERGESORT( $S$ )

# Pick the final pivots: Every  $t$ th element of  $S$ 
 $F[pid] = A[pid \cdot t]$ 

# Determine the rank of each pivot in each substream
 $c = 1$ 
FOR  $i$  in  $0 \dots (n - 1)$  DO
  IF  $I_{pid}[i] > F[c]$  THEN
     $T[pid \cdot P + i] = pid \cdot n + i$ 
    WHILE  $I_{pid}[i] > F[c]$  DO  $c = c + 1$ 

# Calculate target substream offsets (sum entries of each bucket, run prefix sums)
 $B[pid] = (T[0 \cdot P + pid + 1] - T[0 \cdot P + pid]) + \dots + (T[(P - 1) \cdot P + pid + 1] - T[(P - 1) \cdot P + pid])$ 

EXCLUSIVE-PREFIX-SUMS( $B$ )

# Sort substreams by bucket
 $oc = B[pid]$ 
FOR  $i$  in  $0 \dots (P - 1)$  DO
   $O[oc \dots (oc + (T[pid + i \cdot P + 1] - T[pid + i \cdot P]))] =$ 
     $I[T[pid + i \cdot P]] \dots I[T[pid + i \cdot P + 1] - 1]$ 
   $Q[pid \cdot P + i] = oc$ 
   $oc = (oc + (T[pid + i \cdot P + 1] - T[pid + i \cdot P]))$ 
```
